

## Phloroglucinols with Prooxidant Activity from *Garcinia subelliptica*

Chien-Chang Wu,<sup>†</sup> Yi-Huang Lu,<sup>†</sup> Bai-Luh Wei,<sup>‡</sup> Shyh-Chyun Yang,<sup>\*,†</sup> Shen-Jen Won,<sup>§</sup> and Chun-Nan Lin<sup>\*,†</sup>

School of Pharmacy, Kaohsiung Medical University, Kaohsiung 807, Taiwan, Republic of China, Institute of Life Science, National Taitung University, Taitung 950, Taiwan, Republic of China, and Department of Microbiology and Immunology, National Cheng Kung University, Tainan 701, Taiwan, Republic of China

Received September 21, 2007

A new phloroglucinol, garcinielliptone HF (**1**), possessing an unprecedented skeleton, and the tautomeric pair of garcinielliptone FC (**2/2a**) were isolated from the heartwood and pericarp of *Garcinia subelliptica*, respectively. Their structures, including relative configurations, were elucidated by means of spectroscopic methods. The ability of compounds **1** and **2/2a** to induce DNA-cleavage activity was examined using supercoiled plasmid pBR322 DNA. In the presence of Cu(II), compounds **1** and **2/2a** caused significant breakage of pBR322 DNA. The involvement of H<sub>2</sub>O<sub>2</sub> and O<sub>2</sub><sup>•-</sup>, and H<sub>2</sub>O<sub>2</sub>, O<sub>2</sub><sup>•-</sup>, and OH<sup>•</sup> in **1**- and **2/2a**-mediated scission, respectively, was established by inhibition or no protection of DNA breakage by various oxygen radical scavengers. Thus, in the presence Cu(II), **1** and **2/2a** may show a prooxidant effect on DNA and induce cell death.

The isolation and characterization of various compounds including bioactive constituents of *Garcinia subelliptica* Merr. (Clusiaceae) have been reported.<sup>1</sup> Recently, a cytotoxic phloroglucinol, garcinielliptone FB, and 2,4,5-prenylated phloroglucinols with prooxidant activity were isolated from the pericarp and heartwood of this plant.<sup>2,3</sup>

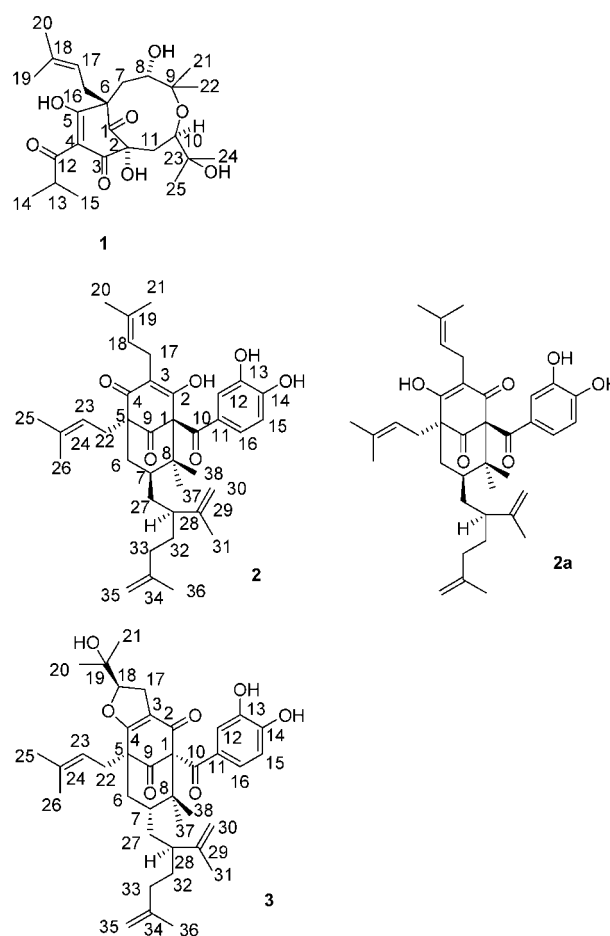
Continued investigation of constituents with prooxidant activity from this plant led to the isolation of a new phloroglucinol, garcinielliptone HF (**1**), possessing an unprecedented skeleton, and the tautomeric pair garcinielliptone FC (**2/2a**) from the heartwood and pericarp of this plant, respectively. Here, the structure elucidation of **1** and **2/2a** and prooxidant effect on DNA damage by **1** and **2/2a** in the presence of Cu(II) are reported.

### Results and Discussion

Compound **1** was isolated as a colorless oil, [ $\alpha$ ]<sub>D</sub><sup>25</sup> –16.7 (*c* 0.22, acetone). The IR spectrum of **1** exhibited absorption bands for hydroxy (3422 cm<sup>-1</sup>), carbonyl (1743 cm<sup>-1</sup>), and  $\alpha,\beta$ -unsaturated  $\beta$ -hydroxy ketone (1603 cm<sup>-1</sup>)<sup>4</sup> moieties. It exhibited a molecular formula of C<sub>25</sub>H<sub>38</sub>O<sub>8</sub> as determined by HRESIMS (*m/z* 471.2358 [M + Na – H<sub>2</sub>O]<sup>+</sup>,  $\Delta$  0.0001 mmu).

The structure of **1** was assigned by a combination of one- and two-dimensional NMR methods. Its <sup>1</sup>H NMR spectrum (Table 1) contained the signals for two secondary methyls, six tertiary methyls, three methylene groups, and four methine groups including two oxymethines. Its <sup>13</sup>C NMR spectrum (Table 1) further indicated the presence of eight methyl, three methylene, four methine, and 10 quaternary carbons.

Analysis of <sup>1</sup>H–<sup>1</sup>H COSY and HMQC spectra of **1** established the connectivities of five <sup>1</sup>H–<sup>1</sup>H and <sup>1</sup>H–<sup>13</sup>C spin systems represented as bold lines (Figure S11, Supporting Information). The HMBC correlations of Me-14/C-12 and Me-15/C-12 together with the IR spectrum, exhibiting an  $\alpha,\beta$ -unsaturated  $\beta$ -hydroxy ketone moiety, established that a 1-oxoisobutyl and a hydroxy group were linked at C-4 and C-5, respectively, and confirmed the linkage between C-4 and C-5. The HMBC correlations of Me-19/C-20, Me-20/C-19, Me-19, and Me-20/C-18, H-17/C-19 and C-20, H $_{\alpha}$ -16/C-18, C-6, C-1, and C-5, and H $_{\beta}$ -16/C-1, and NOESY cross-peaks between Me-19/Me-14 and Me/15 and between Me-20/Me-14



established that a prenyl group was linked at C-6 and confirmed the linkages between C-5/C-6 and C-6/C-1. The HMBC correlation of H $_{\beta}$ -7/C-5 and C-6 confirmed the linkage between C-7 and C-6. The HMBC correlations of H $_{\beta}$ -7/C-9, Me-21/C-22, Me-22/C-21 and Me-21, and Me-22/C-9 and C-8 established that C-21, C-22, and oxygenated C-8 were linked at oxygenated C-9 and a hydroxy group was present at C-8. The HMBC correlations of Me-24/C-25, Me-25/C-24, and Me-24 and Me-25/C-23 and C-10 confirmed that a 2-hydroxyisopropyl group was linked at oxygenated C-10. The HMBC correlations of H $_{\alpha}$ -11/C-1 and C-3 and H $_{\beta}$ -11/C-1 and C-3 and NOESY correlation of OH-2/H-10, with C-2, an oxygenated

\* To whom correspondence should be addressed. Tel: +886 7 3121101. Fax: +886 7 5562365. E-mail: lincna@cc.kmu.edu.tw (Lin); scyang@kmu.edu.tw (Yang).

<sup>†</sup> Kaohsiung Medical University.

<sup>‡</sup> National Taitung University.

<sup>§</sup> National Cheng Kung University.

**Table 1.**  $^1\text{H}$  and  $^{13}\text{C}$  NMR Data of **1** and **2/2a** (in  $\text{CDCl}_3$ )

	<b>1</b>			<b>2</b>		<b>2a</b>	
	$\delta_{\text{H}}$	$\delta_{\text{C}}$	HMBC	$\delta_{\text{H}}$	$\delta_{\text{C}}$	$\delta_{\text{H}}$	$\delta_{\text{C}}$
1		211.9	2.69 ( $\text{H}_{\beta}$ -16), 2.45 ( $\text{H}_{\alpha}$ -16)		69.1		65.5
2		92.6		17.57 (OH)	194.0	17.63 (OH)	198.1
3		210.8	2.69 ( $\text{H}_{\alpha}$ -11), 2.81 ( $\text{H}_{\beta}$ -11)		116.0		116.3
4		124.2			198.1		194.2
5		167.8	2.45 ( $\text{H}_{\alpha}$ -16), 2.04 ( $\text{H}_{\beta}$ -7)		57.8		62.0
6		55.1	1.69 ( $\text{H}_{\alpha}$ -7), 2.04 ( $\text{H}_{\beta}$ -7) 2.45 ( $\text{H}_{\alpha}$ -16), 5.01 (H-17)	$\alpha$ 2.07 (bd, 13.9) $\beta$ 2.37 (bd, 13.9) 1.45 (m)	42.6	$\alpha$ 2.07 (bd, 13.9) $\beta$ 2.37 (bd, 13.9) 1.45 (m)	42.6
7	$\alpha$ 1.69 (dd, 12.8, 12.0) $\beta$ 2.04 (dd, 12.8, 4.6)	33.3			46.8		46.7
8	4.08 (dd, 12.0, 4.6)	68.6	1.69 ( $\text{H}_{\alpha}$ 7), 2.04 ( $\text{H}_{\beta}$ -7) 1.29 (Me-21), 1.59 (Me-22)		49.6		49.4
9		88.1	2.04 ( $\text{H}_{\beta}$ -7), 1.29 (Me-21), 1.59 (Me-22)		209.2		209.3
10	4.40 (t, 7.1)	84.8	2.69 ( $\text{H}_{\alpha}$ 11), 1.10 (Me-24), 1.23 (Me-25)		195.8		195.9
11	$\alpha$ 2.69 (dd, 14.2, 8.2) $\beta$ 2.81 (dd, 14.2, 7.1)	38.3			128.3		128.3
12		200.8	1.01 (Me-14), 1.07 (Me-15)	7.03 (d, 1.7)	116.5	7.10 (d, 1.7)	116.3
13	3.41 m	39.1		8.13 (OH)	143.4	8.13 (OH)	143.4
14	1.01 d (6.9)	17.1	3.40 (H-13)	8.94 (OH)	149.4	8.94 (OH)	149.4
15	1.07 d (6.9)	19.7	3.40 (H-13)	6.67 (d, 8.2)	114.4	6.79 (d, 8.2)	114.4
16	$\alpha$ 2.45 dd (14.2, 7.2) $\beta$ 2.69 dd (14.2, 7.7)	35.2		7.01 (dd, 8.2, 1.7)	124.3	7.06 (dd, 8.2, 1.7)	123.9
17	5.01 t (7.2)	118.6	1.60 (Me-20), 1.65 (Me-19)	$\alpha$ 2.58 (bd, 13.6) $\beta$ 2.74 (bd, 13.6) 5.09 (t, 7.2)	26.4	$\alpha$ 2.58 (bd, 13.6) $\beta$ 2.75 (bd, 13.6) 5.04 (t, 7.2)	26.4
18		136.6	1.60 (Me-20), 1.65 (Me-19), 2.45 ( $\text{H}_{\alpha}$ -16)		120.2		122.7
19	1.65 s	26.1	1.60 (Me-20)		135.1		135.0
20	1.60 s	17.9	1.65 (Me-19)	1.80 (s)	26.1	1.80 (s)	26.1
21	1.29 s	18.7	1.59 (Me-22)	1.73 (s)	17.9	1.72 (s)	17.8
22	1.59 s	27.5	1.29 (Me-21)	$\alpha$ 1.99 (14.5, 7.2) $\beta$ 2.16 (14.5, 8.0)	36.5	$\alpha$ 1.95 (14.5, 7.2) $\beta$ 2.14 (14.5, 8.0)	36.2
23		71.4	2.69 ( $\text{H}_{\alpha}$ -11), 1.10 (Me-24), 1.23 (Me-25)	4.91 (t, 7.2)	123.9	4.84 (t, 7.2)	124.3
24	1.10 s	25.6	1.23 (Me-25)		132.9		132.0
25	1.23 s	26.2	1.10 (Me-24)	1.70 (s)	22.5	1.71 (s)	22.7
26				1.53 (s)	17.7	1.55 (s)	17.5
27				1.88 (2H, m)	31.9	1.95 (2H, m)	32.6
28				2.64 (bd, 13.6)	43.6	2.73 (bd, 13.6)	43.6
29					148.1		147.5
30				4.43 (2H, s)	113.2	4.39 (s) 4.43 (s)	112.6
31				1.56	17.1	1.55 (s)	17.1
32				$\alpha$ 1.95 (m) $\beta$ 2.12 (m) 1.88 (2H, m)	31.9	$\alpha$ 1.95 (m) $\beta$ 2.12 (m) 1.88 (2H, m)	29.1
33					35.5		36.2
34					146.0		146.2
35				4.64 (s) 4.66 (s)	109.6	4.64 (s) 4.66 (s)	109.6
36				1.69 (s)	25.8	1.68 (s)	25.7
37				1.00 (s)	27.0	1.04 (s)	27.0
38				1.15 (s)	22.7	1.15 (s)	22.5

quaternary carbon, established that C-1, C-3, C-11, and a hydroxy group were linked at C-2. The NOESY cross-peak between Me-22/Me-25, with C-9 and C-10, two quaternary oxygenated carbons, suggested that C-9 and C-10 were linked via an oxygen atom. The above results confirmed the linkage between the quaternary C-3 and C-4. This demonstrated that **1** possessed an unprecedented 4-oxabicyclo[6.3.1]dodec-9-ene-11,12-dione skeleton. The NOESY cross-peaks between  $\text{H}_{\beta}$ -7/H-8, H-8/ $\text{H}_{\beta}$ -16,  $\text{H}_{\alpha}$ -11/H-10, H-10/OH-2, Me-19/Me-14 and Me-15, and Me-20/Me-14 suggested that OH-2, OH-8, and H-10 are  $\alpha$ -oriented and that the C-6 prenyl group is  $\beta$ -oriented. Thus the chemical structure of garcinielliptone HF (**1**) was characterized as 1,6,9-trihydroxy-3-(1-hydroxy-1-methylethyl)-10-isobutyryl-5,5-dimethyl-8-(3-methylbut-2-enyl)-4-oxabicyclo[6.3.1]dodec-9-ene-11,12-dione.

From the  $^1\text{H}$  NMR, COSY, and NOESY spectra (Figures S3, S6, and S7, Supporting Information), a computer-generated 3D structure (Figure S10, Supporting Information) of **1** was obtained. The calculated distances between  $\text{H}_{\beta}$ -7/H-8 (2.220 Å),  $\text{H}_{\beta}$ -16/H-8

(3.965 Å),  $\text{H}_{\alpha}$ -11/H-10 (2.210 Å), H-10/OH-2 (2.453 Å), Me-19/Me-15 (2.428 Å), Me-19/Me-14 (3.993 Å), and Me-20/Me-14 (3.253 Å) are all less than 4 Å. This is consistent with the well-defined NOESY interactions observed for each of these proton pairs. The presence of significant peaks at  $m/z$  487 [ $\text{M} + \text{Na} - 2\text{H}$ ] $^+$ , 471 [ $\text{M} - \text{H}_2\text{O} + \text{Na}$ ] $^+$ , 449 [ $\text{M} - \text{H}_2\text{O} + \text{H}$ ] $^+$ , and 381 [ $449 - (\text{CH}_3)_2\text{C}=\text{CH} - \text{Me} + 2\text{H}$ ] $^+$  in the positive ESIMS also supported the structure of **1**.

The molecular formula of **2/2a**, [ $\alpha$ ] $^{25}\text{D}$  12.6 ( $c$  1.0,  $\text{CHCl}_3$ ), was determined as  $\text{C}_{38}\text{H}_{50}\text{O}_6$  by HRESIMS ( $[\text{M} + 1]^+$ ,  $m/z$  603.3684,  $\Delta$  0.0001 mmu), which was consistent with its  $^1\text{H}$  and  $^{13}\text{C}$  NMR data. The IR absorption of **2/2a** implied the presence of OH ( $3390\text{ cm}^{-1}$ ), conjugated ketone ( $1727\text{ cm}^{-1}$ ), and aromatic ( $1605\text{ cm}^{-1}$ ) moieties. The UV spectrum indicated the presence of a conjugated aromatic moiety [ $\lambda_{\text{max}}$  275 (4.37) and 208 (4.58) nm]. The  $^1\text{H}$  NMR spectrum of **2/2a** (Table 1) revealed the presence of resonances for four  $\gamma,\gamma$ -dimethylallyl groups, two 2-isopropenylhex-5-enyl groups, four tertiary methyls, two methylenes, and two aromatic

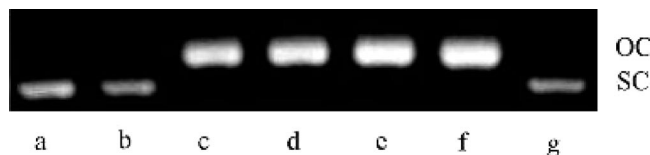


**Figure 1.** Agarose gel electrophoretic patterns of plasmid DNA treated with **1** in the presence of Cu(II) ion. pBR322 plasmid DNA (500 ng) was incubated for 30 min at 37 °C in the presence of the following additives: (a) no addition (DNA control); (b) Cu(II) (300 μM); (c–g) 300, 200, 100, 50, 25 μM **1** + Cu(II) (300 μM).

ABX systems. The  $^1\text{H}$  NMR spectrum in acetone- $d_6$  indicated the presence of four phenolic protons at  $\delta$  8.13 (s, 2H) and 8.94 (s, 2H) and two unusually low-field-shifted signals ( $\delta$  17.57, 17.63, each br s) indicating the presence of strongly hydrogen-bonded hydroxy protons. The  $^{13}\text{C}$  NMR showed signals of 76 carbons, which could be sorted by DEPT experiments into 16 methyl, 16 methylenes, 14 methines, and 30 quaternary carbons including six carbonyl groups ( $\delta_{\text{C}}$  194.9, 195.0, 198.7, 198.9, 209.2, 209.3) and two carbons substituted by enolic hydroxy groups ( $\delta$  194.0, 194.2) (for  $^{13}\text{C}$  NMR data, see Table 1). However, duplicated  $^1\text{H}$  and  $^{13}\text{C}$  NMR patterns in a ratio of approximately 5:1 (derived from the  $^1\text{H}$  NMR signal intensity) and only one pseudomolecular ion peak in the positive HRESIMS demonstrated that the compound exists in isomeric forms. This was later shown to be the two enolic tautomers **2** and **2a** in solution ( $\text{CDCl}_3$ ), with **2** being the preferred tautomer. The assignment of the structure presented refers to the preferred tautomeric structure **2**.

In the  $^1\text{H}$  and  $^{13}\text{C}$  NMR of **2**, the chemical shift values of a prenyl group, a 2-isopropenylhex-5-enyl group, two tertiary methyls, a methylene, and an aromatic ABX system were similar to those of corresponding data of garcinelliptone FB (**3**).<sup>2</sup> The carbon signals of C-1 and C-5 to C-9 were also similar to those of corresponding data of **3**.<sup>2</sup> The HMBC correlations (Figure S11, Supporting Information) of Me-20/C-19 and C-21, Me-21/C-19 and C-18, and H $_{\beta}$ -17/C-3 and the  $^1\text{H}$ – $^1\text{H}$  COSY (Figure S11, Supporting Information) correlation between H-18/H-17 established a prenyl group linked at C-3. The unusually low-field-shifted phenolic proton at  $\delta$  17.57 indicated NOSEY correlations with phenolic protons at  $\delta$  8.13 and 8.94, respectively. This revealed that the enolic hydroxy group was substituted at C-2 and that a quaternary carbonyl carbon was located between C-3 and C-5. The HMBC correlation of OH-C-13/C-12 suggested that the protons at  $\delta$  8.13 and 8.94 could be assigned to the phenolic C-13 and C-14 protons, respectively.

NOESY cross-peaks of H-7/H $_{\alpha}$ -6, H $_{\alpha}$ -22, Me-37, and H-28 suggested that the prenyl groups at C-5, H-7, H-28, and Me-37 are  $\alpha$ -oriented. In the  $^{13}\text{C}$  NMR spectrum of **2**, the chemical shift value of C-1 ( $\delta$  69.1) was significantly different from that of the corresponding carbon ( $\delta$  78.9) of **3**.<sup>2</sup> This suggested that the benzoyl group at C-1 is  $\beta$ -oriented. Therefore, compound **2** was characterized as 8,8-dimethyl-1-(3,4-dihydroxybenzoyl)-2-hydroxy-3,5-di( $\gamma,\gamma$ -dimethylallyl)-7-(2-isopropenylhex-5-enyl)-7 $\alpha$ -H-trans-bicyclo[3.3.1]nona-2-en-4,9-dione (**2**). The tautomeric form **2a** was identified as 8,8-dimethyl-1-(3,4-dihydroxybenzoyl)-4-hydroxy-3,5-di( $\gamma,\gamma$ -dimethylallyl)-7-(2-isopropenylhex-5-enyl)-7 $\alpha$ -H-trans-bicyclo[3.3.1]nona-3-en-2,9-dione (**2a**).

Compounds **1** and **2/2a** were tested for converting supercoiled plasmid pBR322 DNA to relaxed open circles in the presence of Cu(II). As shown in Figures 1 and 2, compounds **1** and **2/2a** gave a significant level of Cu(II)-mediated DNA breakage reaction in a concentration-dependent manner. Compound **1** at 300 to 50 μM and **2/2a** at 300 and 200 μM significantly converted the supercoiled (SC) DNA to open circle (OC) DNA in the Cu(II)-mediated DNA breakage reaction, respectively.

As shown in Figure 3, the conversion of supercoiled DNA to relaxed form induced by **1** and **2/2a** in the presence of Cu(II) was

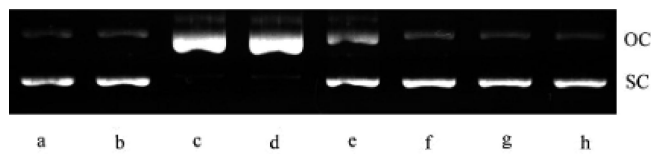


**Figure 2.** Agarose gel electrophoretic patterns of plasmid DNA treated with **2/2a** in the presence of Cu(II) ion. pBR322 plasmid DNA (500 ng) was incubated for 30 min at 37 °C in the presence of the following additives: (a) no addition (DNA control); (b) Cu(II) (300 μM); (c–h) 300, 200, 100, 50, 25, 10 μM **2/2a** + Cu(II) (300 μM).

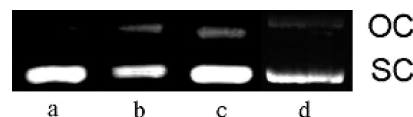


**Figure 3.** Effect of neocuproine (600 μM) on **1**- and **2/2a** (300 μM)–Cu(II) (300 μM)-induced breakage of pBR322 DNA: (a) DNA alone; (b) DNA + Cu(II) + neocuproine; (c) DNA + Cu(II) + **1** + neocuproine; (d) DNA + Cu(II) + **2/2a** + neocuproine.

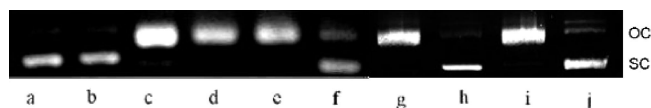


**Figure 4.** Effect of active oxygen scavengers on **1**- and **2/2a**–Cu(II)-mediated DNA breakage: (a) DNA alone; (b) DNA + Cu(II) (300 μM); (c) DNA + **1** (300 μM) + Cu(II) (300 μM); (d–f) same as (c) with potassium iodide (750 μM), superoxide dismutase (0.1 mg/mL), and catalase (0.1 mg/mL), respectively; (g) DNA + **2/2a** (300 μM) + Cu(II) (300 μM); (h–j) same as (g) with potassium iodide (750 μM), superoxide dismutase (0.1 mg/mL), and catalase (0.1 mg/mL), respectively.

inhibited with neocuproine (600 μM), a Cu(I)-specific sequestering agent.<sup>5</sup> This suggested that Cu(I) is the essential intermediate in the **1**- and **2/2a**-mediated DNA cleavage reaction.

The **1**- and **2/2a**–Cu(II)-mediated DNA breakage reaction was further tested for inhibition by various oxygen radical scavengers. As shown in Figure 4, **1**- and **2/2a**–Cu(II)-induced DNA degradation was inhibited by catalase and revealed DNA breakage by KI and superoxide dismutase (SOD) and inhibition of DNA breakage by catalase and KI and revealed DNA breakage by SOD, respectively. This indicated that  $\text{H}_2\text{O}_2$  and  $\text{O}_2^{\cdot-}$ , and  $\text{H}_2\text{O}_2$ ,  $\text{OH}^{\cdot}$ , and  $\text{O}_2^{\cdot-}$  appeared to be involved in the **1**- and **2/2a**–Cu(II)-mediated DNA breakage reaction.

The effect of **2/2a** on the viability of MCF-7 cells was examined by flow cytometry analysis. MCF-7 cells were treated with different concentrations of **2/2a** for different time periods. As shown in Figure 5, a sub- $G_1$  peak was detected in the DNA histograms of **2/2a** at various concentrations for different time periods. The shift of  $G_0/G_1$  and  $G_2/M$  cell cycles to the sub- $G_1$  phase is increased dose-dependently in the MCF-7 cells for different time periods. However a maximum 47.6% apoptotic cells was detected at 72 h. Within various time periods, Hoechst 33258 staining of cells exposed to various concentrations of **2/2a** demonstrated typical morphological changes of apoptosis (Figure 6). The cells shrank, turned round, and had a relatively smaller volume than control cells. Chromatin DNA was extensively condensed and DNA was fragmented. The typical morphological and biochemical features clearly revealed that **2/2a** causes cell death by apoptosis.

Compound **2/2a**, with a catechol moiety, may participate in redox cycling. In the presence of Cu(II), **2/2a** caused breakage of supercoiled plasmid pBR322 DNA, while **3** did not. This indicated that the enolic hydroxy group at C-2 of **2** or C-4 of **2a** and the

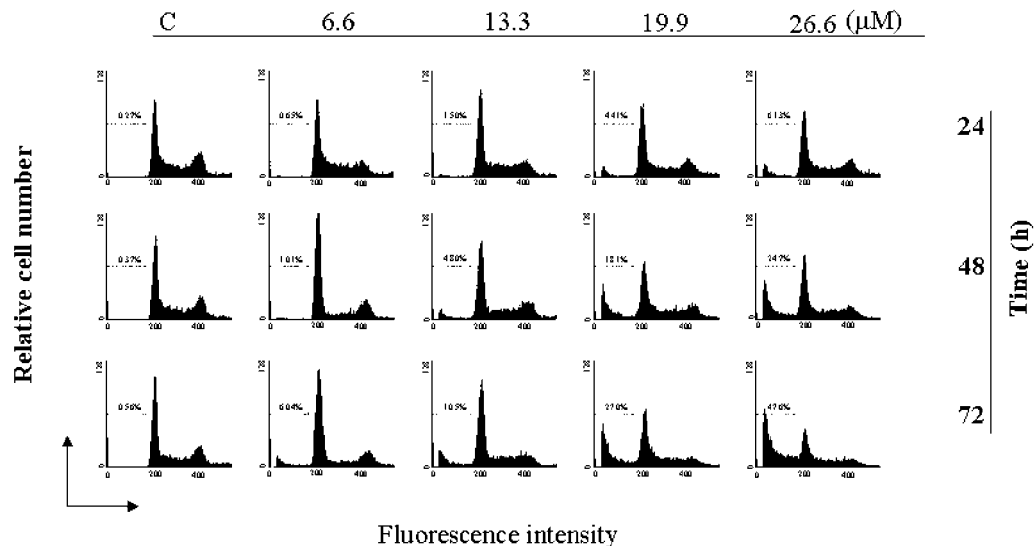


**Figure 5.** Flow cytometry analysis of **2/2a**-treated MCF-7 cells. MCF-7 cells ( $1 \times 10^4$  cells/mL) were treated with various concentrations of **2/2a** for different time periods. At the times indicated, cells were stained with propidium iodide (PI), and DNA contents were analyzed by flow cytometry; apoptosis was measured by the accumulation of sub-G<sub>1</sub> DNA contents in cells. The control cells were treated with medium. Results are representative of three independent experiments.

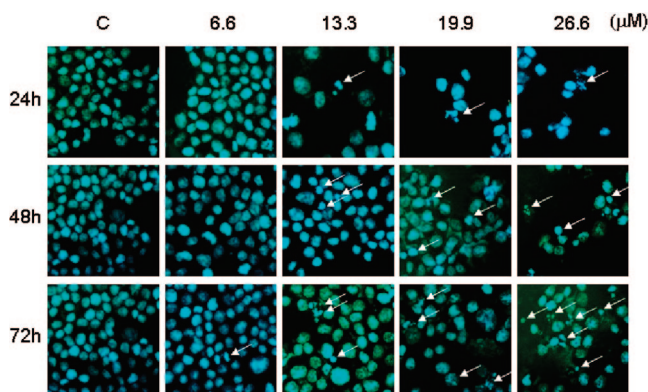


**Figure 6.** Fluorescence microscopy observation of chromatin condensation in MCF-7 cells induced by **2/2a**. Costaining of Hoechst 33258 and PI showed shrunken nuclei and nuclear fragmentation in MCF-7 cells treated with **2/2a** (6.6, 13.3, 19.9, and 26.6  $\mu\text{M}$ ). The control cells (C) were treated with medium.

carbonyl group at C-4 of **2** or C-2 of **2a** were necessary for Cu(II)-mediated DNA damage.

In the presence or absence of a low concentration Cu(II) (400 ng/mL), the inhibitory effect of **2/2a** on the viability of MCF-7 cells was also examined by flow cytometry analysis. In the presence of Cu(II) (400 ng/mL) in MCF-7 cells cotreated with **2/2a** (18  $\mu\text{g}/\text{mL}$ ) for 48 h a sub-G<sub>1</sub> peak was detected in DNA histograms (C and D, Figure 7). The shift of G<sub>0</sub>/G<sub>1</sub> and G<sub>2</sub>/M cell cycles to the sub-G<sub>1</sub> phase increased. This clearly indicated that cupric ion potentiated the **2/2a**-induced cell death by apoptosis. Compound **2/2a** cotreated with Cu(II) (800 ng/mL) in MCF-7 cells showed a significant increase of apoptosis (data not shown) compared with that of **2/2a** cotreated with Cu(II) (400 ng/mL) in MCF-7 cells. Incubation with 10  $\mu\text{M}$  Cu(II) in trout hepatocytes resulted in a strong stimulation of reactive oxygen species (ROS) formation and a significant increase of both apoptotic and necrotic cells,<sup>6</sup> while MCF-7 cells treated with 400 ng/mL Cu(II) did not induce apoptosis (Figure 7). In the presence of higher concentrations of Cu(II), MCF-7 cells cotreated with **2/2a** may enhance the formation of ROS induced by Cu(II) and significantly increase apoptosis in MCF-7 cells. Additional studies will be required to elucidate the

molecular mechanism of **2/2a** on human MCF-7 cells with and without copper.

#### Experimental Section

**General Experimental Procedures.** Optical rotations were recorded with a JASCO-370 polarimeter using acetone as solvent. UV spectra were obtained on a JASCO model 7800 UV-vis spectrophotometer. IR spectra were measured on a Perkin-Elmer 2000 FT-IR spectrophotometer. <sup>1</sup>H (400 MHz) and <sup>13</sup>C NMR (100 MHz) spectra were recorded on Varian-Unity-400 NMR spectrophotometer. MS were obtained on a JMS-HX-100 mass spectrometer. Si gel for column chromatography (Merck) particle size 15–40  $\mu\text{m}$  and RP-18 (Nakalai tesque) particle size 75  $\mu\text{m}$  were used for column chromatography. Si gel 60 F<sub>254</sub> precoated aluminum sheets (0.2 mm, Merck) and RP 18 F<sub>254</sub> precoated sheets (0.25 mm, Merck) were used for TLC controls. All solvents were of HPLC grade. Ethidium bromide, bromophenol blue, and Trizma were purchased from Sigma Chemicals. EDTA disodium salt was purchased from J. T. Baker; CuCl<sub>2</sub> and glycerol were from Mallinckrodt, Inc. Supercoiled pBR322 plasmid DNA was purchased from ABgene, Advanced Biotechnologies Ltd., UK.

**Plant Material.** The heartwood of *Garcinia subelliptica* (10 kg) was collected at Ping-Tung Hsien, Taiwan, in August 2004 and authenticated by Dr. Ming-Hong Yen, School of Pharmacy, Kaohsiung Medical University. A voucher specimen (2004-GH) is deposited in the Laboratory of Medicinal Chemistry, School of Pharmacy, Kaohsiung Medical University. The fresh pericarps of *G. subelliptica* (15.3 kg) were collected at Kaohsiung, Taiwan, in July 2001. A voucher specimen (2001-3) has been deposited at the Department of Medicinal Chemistry, School of Pharmacy, Kaohsiung Medical University.

**Extraction and Isolation.** The heartwood of *G. subelliptica* (10 kg) was chipped and extracted with CH<sub>2</sub>Cl<sub>2</sub> at room temperature. The resultant CH<sub>2</sub>Cl<sub>2</sub> extract (100 g) was chromatographed over a Si gel column and eluted with *n*-hexane containing increasing amounts of EtOAc and final washing with MeOH to yield 33 fractions. Fraction 22 was further purified on a RP18 column eluted with acetone–H<sub>2</sub>O (1:1) to yield **1** (44.5 mg). The fresh pericarp of *G. subelliptica* (15.3 kg) was extracted with CHCl<sub>3</sub> at room temperature. The CHCl<sub>3</sub> extract was concentrated under reduced pressure to afford a brown residue (196 g). The residue (196 g) was fractionated by chromatography over Si gel, using *n*-hexane–EtOAc (19:1), *n*-hexane–EtOAc (9:1), *n*-hexane–EtOAc (4:1), and *n*-hexane–EtOAc (2:1), to afford fractions A, B, C, and D. Fraction C was chromatographed over Si gel, and elution with *n*-hexane–acetone (2:1) yielded **2/2a** (100 mg).

**Garcinelliptone HF (1):** colorless oil;  $[\alpha]_D^{25} -16.7$  (*c* 0.22, acetone); UV (MeOH)  $\lambda_{\text{max}}$  (log  $\epsilon$ ) 244 (4.13) nm; IR (KBr) 3422, 1743, 1603  $\text{cm}^{-1}$ ; <sup>1</sup>H and <sup>13</sup>C NMR spectral data, see Table 1; ESIMS (positive) *m/z* 487 [M + Na – 2H]<sup>+</sup>, 471 [M + Na – H<sub>2</sub>O]<sup>+</sup>, 449 [M

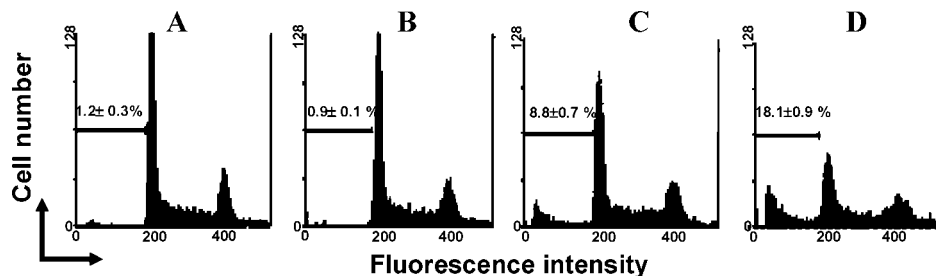


**Figure 7.** Flow cytometry analysis of **2/2a** (with and without copper)-treated MCF-7 cells. MCF-7 ( $1 \times 10^5$  cells/mL) were untreated (A and B with  $\text{Cu}^{2+}$ , 400 ng/mL) or treated with **2/2a** (18  $\mu\text{g/mL}$ ) (C and D with  $\text{Cu}^{2+}$ , 400 ng/mL) for 48 h. After incubation for 48 h, cells were stained with propidium iodide (PI), and DNA contents were analyzed by flow cytometry. Apoptosis was measured by the accumulation of sub- $G_1$  DNA content in cells. The control cells were treated with medium. Results are representative of three independent experiments.

–  $\text{H}_2\text{O} + \text{H}^+$ , 381 [449 –  $(\text{CH}_3)_2\text{C}=\text{CH}^- - \text{Me} + 2\text{H}^+$ ]; HRESIMS: 471.2358 for  $\text{C}_{25}\text{H}_{36}\text{O}_7\text{Na}$  (471.2359,  $\Delta$  0.0001 mmu).

**Garcinielliptone FC (2/2a):** yellow oil;  $[\alpha]_D^{25}$  12.6 (c 1.0,  $\text{CHCl}_3$ ); UV (MeOH)  $\lambda_{\text{max}}$  (log  $\epsilon$ ) 275 (4.37) and 208 (4.58) nm; IR (KBr)  $\nu_{\text{max}}$  1605, 1727, 3390  $\text{cm}^{-1}$ ;  $^1\text{H}$  NMR (acetone- $d_6$ , 400 MHz) and  $^{13}\text{C}$  NMR (acetone- $d_6$ , 100 MHz), see Table 1; EIMS  $m/z$  602  $[\text{M}]^+$  (3), 465 (4), 137 (75), 95 (22), 69 (100); HRESIMS  $m/z$   $[\text{M} + 1]^+$  603.3684 (calcd for  $\text{C}_{38}\text{H}_{50}\text{O}_6$ , 603.3685).

**DNA Strand Scission Assay.** Reaction mixtures (25  $\mu\text{L}$ ) contained 10 mM Tris-HCl (pH 8.0), supercoiled pBR322 plasmid DNA (500 ng), compound **1**, and **2/2a** (each dissolved in DMSO, with the final DMSO concentration being no more than 5% in the 25  $\mu\text{L}$  reaction solution) and other components as described in the figure legends. After incubation at 37  $^\circ\text{C}$  for 30 min, the reaction mixture was treated with 5  $\mu\text{L}$  of 30% glycerol–0.01% bromophenol blue and was analyzed by electrophoresis in a 1.0% agarose gel containing 0.7  $\mu\text{g/mL}$  ethidium bromide. The electrophoresis was carried out in TBE buffer (89 mM Tris, 89 mM boric acid containing 2 mM EDTA, pH 8.3) at 110 V for 45 min. Following electrophoresis, the gel was viewed and photographed on a UV transilluminator.<sup>5</sup>

**Flow Cytometry.** Compounds with and without  $\text{Cu}^{2+}$  were added to cells ( $1 \times 10^7$ ), respectively. At various time intervals, the reactions were terminated by washing with PBS. The cells were fixed with 4% paraformaldehyde/PBS (pH 7.4) at room temperature for 30 min. After centrifugation at 1000 rpm for 10 min, the cells were permeabilized with 0.1% Triton-X–100/0.1% sodium citrate at 4  $^\circ\text{C}$  for 2 min. The intensity of the fluorescence was measured with a FACScan flow cytometer (Becton Dickinson, Mountain View, CA). A minimum of 5000 cell counts were collected for the analysis by LYSIS II Software.

**Fluorescence Observation.** Morphological changes of the cells were observed directly in culture vehicles. To observe chromatin condensa-

tion and plasma membrane permeability, cells were resuspended in fresh culture medium after collection by centrifugation, costained propidium iodide (PI, 0.05  $\text{g/L}$ ) and Hoechst 33258 (0.01  $\text{g/L}$ ) at 37  $^\circ\text{C}$  for 30 min, then centrifuged to remove most of the supernatant. The pellet was suspended in the remaining culture medium and smeared for fluorescence microscopy.

**Acknowledgment.** This work was supported by a grant from the National Science Council of the Republic of China (NSC 94-2320-B-037-033).

**Supporting Information Available:** Figures showing substructures (bold lines) and HMBC correlations of **1** and **2**, selective NOESY correlations and relative configuration of **1**, and 1D and 2D NMR spectra of **1** are available free of charge via the Internet at <http://pubs.acs.org>.

## References and Notes

- Weng, J. R.; Tsao, L. T.; Wang, J. P.; Wu, R. R.; Lin, C. N. *J. Nat. Prod.* **2004**, *67*, 1796–1799.
- Wu, C. C.; Weng, J. R.; Won, S. J.; Lin, C. N. *J. Nat. Prod.* **2005**, *68*, 1125–1127.
- Lu, Y. H.; Wei, B. L.; Ko, H. H.; Lin, C. N. *Phytochemistry* **2007**, doi: (10.1016/j.phytochem.2007.06.026).
- Bellamy, L. J. *The Infra-Red Spectra of Complex Molecules*, 2nd ed.; Methuen & Co Ltd.: London, 1958; p 132.
- Ahsan, H.; Hadi, S. M. *Cancer Lett.* **1998**, *124*, 23–30.
- Krumshnabel, G.; Manzl, C.; Berger, C.; Hofer, B. *Toxicol. Appl. Pharmacol.* **2005**, *209*, 62–73.

NP070507O